High index contrast semiconductor ARROW and hybrid ARROW fibers

N. Healy,[1*] J. R. Sparks,[2] R. R. He,[2] P. J. A. Sazio,[1] J. V. Badding[2] and A. C. Peacock[1]

[1]*Optoelectronics Research Centre, University of Southampton, Southampton, SO17 1BJ, UK*
[2]*Department of Chemistry and Materials Research Institute, Pennsylvania State University,16802 PA, USA*
**nvh@orc.soton.ac.uk*

Abstract: We investigate the guidance properties of two photonic crystal fibers that have been fabricated by filling the holes of a silica template with hydrogenated amorphous silicon inclusions. The first is an all-solid fiber that guides light via an antiresonant reflecting optical waveguiding mechanism and the second is only partially filled so that it guides light by a hybrid of modified total internal reflection and antiresonant reflecting optical waveguiding. It will be shown that, by selectively filling the silica template to leave an unfilled internal ring of holes, the fiber's confinement loss can be reduced significantly. This novel fiber design in which the light guided in the silica core can be modified by the semiconductor cladding provides a route to integrating functional semiconductor fibers with existing silica fiber infrastructures.

©2011 Optical Society of America

OCIS codes: (060.5295) Photonic crystal fibers; (160.6000) Semiconductor materials.

References and links

1. J. C. Knight, T. A. Birks, P. St. J. Russell, and D. M. Atkin, "All-silica single-mode optical fiber with photonic crystal cladding," Opt. Lett. **21**(19), 1547–1549 (1996), http://www.opticsinfobase.org/abstract.cfm?URI=ol-21-19-1547.
2. J. M. Dudley, and J. R. Taylor, "Ten years of nonlinear optics in photonic crystal fibre," Nat. Photonics **3**(2), 85–90 (2009).
3. W. Wadsworth, R. Percival, G. Bouwmans, J. Knight, and P. Russell, "High power air-clad photonic crystal fibre laser," Opt. Express **11**(1), 48–53 (2003), http://www.opticsinfobase.org/abstract.cfm?URI=oe-11-1-48.
4. J. B. Jensen, L. H. Pedersen, P. E. Hoiby, L. B. Nielsen, T. P. Hansen, J. R. Folkenberg, J. Riishede, D. Noordegraaf, K. Nielsen, A. Carlsen, and A. Bjarklev, "Photonic crystal fiber based evanescent-wave sensor for detection of biomolecules in aqueous solutions," Opt. Lett. **29**(17), 1974–1976 (2004), http://www.opticsinfobase.org/abstract.cfm?URI=ol-29-17-1974.
5. R. F. Cregan, B. J. Mangan, J. C. Knight, T. A. Birks, P. St. J. Russell, P. J. Roberts, and D. C. Allan, "Single-mode photonic band gap guidance of light in air," Science **285**(5433), 1537–1539 (1999).
6. N. M. Litchinitser, A. K. Abeeluck, C. Headley, and B. J. Eggleton, "Antiresonant reflecting photonic crystal optical waveguides," Opt. Lett. **27**(18), 1592–1594 (2002), http://www.opticsinfobase.org/abstract.cfm?URI=ol-27-18-1592.
7. N. M. Litchinitser, S. C. Dunn, B. Usner, B. J. Eggleton, T. P. White, R. C. McPhedran, and C. M. de Sterke, "Resonances in microstructured optical waveguides," Opt. Express **11**(10), 1243–1251 (2003), http://www.opticsinfobase.org/abstract.cfm?URI=oe-11-10-1243.
8. A. Fuerbach, P. Steinvurzel, J. Bolger, and B. Eggleton, "Nonlinear pulse propagation at zero dispersion wavelength in anti-resonant photonic crystal fibers," Opt. Express **13**(8), 2977–2987 (2005), http://www.opticsinfobase.org/abstract.cfm?URI=oe-13-8-2977.
9. A. Isomäki, and O. G. Okhotnikov, "Femtosecond soliton mode-locked laser based on ytterbium-doped photonic bandgap fiber," Opt. Express **14**(20), 9238–9243 (2006), http://www.opticsinfobase.org/abstract.cfm?URI=oe-14-20-9238.
10. T. Larsen, A. Bjarklev, D. Hermann, and J. Broeng, "Optical devices based on liquid crystal photonic bandgap fibres," Opt. Express **11**(20), 2589–2596 (2003), http://www.opticsinfobase.org/abstract.cfm?URI=oe-11-20-2589.
11. T. Alkeskjold, J. Lægsgaard, A. Bjarklev, D. Hermann, A. Anawati, J. Broeng, J. Li, and S. T. Wu, "All-optical modulation in dye-doped nematic liquid crystal photonic bandgap fibers," Opt. Express **12**(24), 5857–5871 (2004), http://www.opticsinfobase.org/abstract.cfm?URI=oe-12-24-5857.

#144221 - $15.00 USD Received 16 Mar 2011; accepted 21 Mar 2011; published 20 May 2011
(C) 2011 OSA

12. A. F. Oskooi, J. D. Joannopoulos, and S. G. Johnson, "Zero-group-velocity modes in chalcogenide holey photonic-crystal fibers," Opt. Express **17**(12), 10082–10090 (2009), http://www.opticsinfobase.org/abstract.cfm?URI=oe-17-12-10082.
13. L. Lagonigro, N. Healy, J. R. Sparks, N. F. Baril, P. J. A. Sazio, J. V. Badding, and A. C. Peacock, "Low loss silicon fibers for photonics applications," Appl. Phys. Lett. **96**(4), 041105 (2010).
14. P. Mehta, N. Healy, N. F. Baril, P. J. A. Sazio, J. V. Badding, and A. C. Peacock, "Nonlinear transmission properties of hydrogenated amorphous silicon core optical fibers," Opt. Express **18**(16), 16826–16831 (2010), http://www.opticsinfobase.org/abstract.cfm?URI=oe-18-16-16826.
15. D. J. Won, M. O. Ramirez, H. Kang, V. Gopalan, N. F. Baril, J. Calkins, J. V. Badding, and P. J. A. Sazio, "All-optical modulation of laser light in amorphous silicon-filled microstructured optical fibers," Appl. Phys. Lett. **91**(16), 161112 (2007).
16. H. H. Li, "Refractive index of silicon and germanium and its wavelength and temperature derivatives," J. Phys. Chem. Ref. Data **9**(3), 561–601 (1980).
17. G. P. Agrawal, *Nonlinear Fiber Optics*, 2nd ed. (Academic, San Diego, Calif., 1995).
18. J. M. Stone, G. J. Pearce, F. Luan, T. A. Birks, J. C. Knight, A. K. George, and D. M. Bird, "An improved photonic bandgap fiber based on an array of rings," Opt. Express **14**(13), 6291–6296 (2006), http://www.opticsinfobase.org/abstract.cfm?URI=oe-14-13-6291.
19. R. R. He, P. J. A. Sazio, A. C. Peacock, N. Healy, M. Krishnamurthi, V. Gopalan and J. V. Badding, "Active optical fibres with integrated semiconductor junctions," in preparation.
20. B. T. Kuhlmey, B. J. Eggleton, and D. K. C. Wu, "Fluid-filled solid-core photonic bandgap fibers," J. Lightwave Technol. **27**(11), 1617–1630 (2009), http://www.opticsinfobase.org/abstract.cfm?URI=JLT-27-11-1617.
21. C.-P. Yu, and J. H. Liou, "Selectively liquid-filled photonic crystal fibers for optical devices," Opt. Express **17**(11), 8729–8734 (2009), http://www.opticsinfobase.org/abstract.cfm?URI=oe-17-11-8729.

1. Introduction

Since the first demonstration of the photonic crystal fiber (PCF) in 1996 [1], there have been hundreds of experimental and theoretical iterations that exploit its unique properties for applications ranging from non-linear optics [2], fiber lasers [3], and sensing [4]. The versatility of the PCF is predominantly due to its 2D transverse microstructured cladding that consists of a background material and a lattice of periodic inclusions. The PCF can be classed into two distinct groups, those that guide through the mechanism of modified total internal reflection (TIR) and those that guide through resonant effects associated with the microstructured cladding. The former's guidance mechanism is analogous to the conventional step index fiber, in which the core has a higher refractive index than the cladding, so that either the cladding inclusions or the background material must have a lower refractive index than the core [1].

In general, the second class of fiber has cladding inclusions that are of equal or higher refractive index than that of the core and are well described by the photonic bandgap (PBG) model which considers the guidance mechanism as a series of Bragg reflections induced by the periodic refractive index of the cladding [5]. For the particular case, when the cladding inclusions have a higher refractive index than that of the background material, it has been shown that they can be treated as isolated waveguides and the antiresonant reflecting optical waveguide (ARROW) model serves as a simple alternative to describe the PCF [6]. This model acknowledges that a single dielectric cladding inclusion can support its own guided modes. These modes, or resonances, determine the width and position of the PCF's transmission bands. If light impinging on the inclusion is on resonance with one of its modes then it can propagate through the cladding and escape from the core. Conversely, if the light is off resonance, it is reflected back into the core where it is confined and guided. Litchinister *et al*. demonstrated that for modes of a cylindrical inclusion, a suitable approximation of the resonant and antiresonant wavelengths is given by [7]:

$$\lambda_m \approx \frac{2d\sqrt{(n_{inc}^2 - n_{bg}^2)}}{m+\sigma}, \tag{1}$$

where λ_m is the wavelength, d is the inclusion diameter, m is a positive integer, n_{inc} and n_{bg} are the refractive indices of the inclusion and the background material, respectively. When σ =

#144221 - $15.00 USD Received 16 Mar 2011; accepted 21 Mar 2011; published 20 May 2011
(C) 2011 OSA

1/2, λ is resonant and no core mode is supported and when $\sigma = 0$, λ is antiresonant and light is guided by the core. Thus the position and width of the transmission bands for an ARROW fiber are strongly dependent on the refractive index of the cylindrical inclusions. Also, due to the resonant nature of the ARROW guidance mechanism, the group velocity dispersion of each guidance band tends towards $-\infty$ at longer wavelengths and $+\infty$ at shorter wavelengths and has a zero dispersion wavelength positioned at approximately the band's center wavelength [8]. These properties make ARROW fibers exciting candidates for many useful applications and, indeed, a number of devices have been demonstrated by using various high index cladding inclusions, for example fiber lasers [9], tunable transmission filters [10] and optical modulators [11]. It has also been suggested that zero, or near zero, group velocity modes can exist on PCF fibers that have a large index contrast and such modes could be used to for enhanced light-matter interactions [12].

Another nascent class of optical fiber that offers enhanced functionality is the semiconductor optical fiber [13]. Typically the semiconductor is incorporated as the core of the waveguiding structure where its electronic and optical properties can be easily exploited. A number of unary and binary semiconductor optical fibers have been demonstrated and, thus far, one of the most promising core materials in terms of functionality has been hydrogenated amorphous silicon (a-Si:H). This material has been shown to have enhanced non-linear properties for use in non-linear pulse shaping [14] and all-optical modulation [15]. Compared to pure silica, however, the relatively high material losses are currently limiting the potential applications of these silicon core fibers at telecoms wavelengths.

In this paper, we present the first steps to unite these two emerging fiber classes to produce a structure in which we can exploit the semiconductor's functionality to alter the guidance properties of the ARROW fiber. The light is guided in the low loss silica core of the proposed fiber and an important feature of this design is that these fibers should offer efficient coupling and integration with other more conventional silica core fibers. This is a distinct advantage over the step index semiconductor optical fibers which have high Fresnel reflection losses due to the large refractive index of the semiconductor core. The fibers used in our investigations are fabricated using a high pressure chemical deposition technique to deposit a-Si:H into the holes of a pure silica TIR guiding PCF template so that the cladding now consists of high index inclusions. We will describe two different types of fiber; one in which the template is completely filled with a-Si:H so that the guidance is best described via the ARROW mechanism (i.e. a Si-ARROW fiber), and the second where the ring of holes surrounding the core is left empty so that it guides via a hybrid of TIR and ARROW effects. Numerical modeling is used to support the experimental observations where it will be shown that it is possible to control the confinement loss through the selective filling of the template. The loss values measured in these first generation fibers suggest that they should find application in a range of devices which could benefit from the functionality of the semiconductor inclusions.

2. Si-ARROW fiber

The silica PCF template used in our investigations is shown in Fig. 1(a), with a cladding hole diameter d = 1.17 μm and pitch Λ = 2.15 μm. We start by modeling the Si-ARROW fiber where all the holes are filled with a-Si:H inclusiomns. The a-Si:H material is assumed to have an index of ~3.6 at 1550 nm, however, in practice the refractive index is sensitive to the hydrogen content and can therefore be used to tune the position of the transmission bands. The wavelength dependence of the material refractive indices are included via the appropriate Sellmeier relations [16,17], with the silicon material losses included as measured in Ref [13]. A full vector finite element method (FEM) was used to model the modal properties across a wavelength range of 1300 nm to 1700 nm and the simulated transmission spectrum of the Si-ARROW fiber is shown in Fig. 1(b). This spectrum shows a well-defined band structure, with two distinct guidance bands centered at 1350 nm and 1600 nm, which agree well with the

#144221 - $15.00 USD Received 16 Mar 2011; accepted 21 Mar 2011; published 20 May 2011
(C) 2011 OSA

predictions for the resonant and antiresonant wavelengths of Eq. (1). The simulated group velocity dispersion (GVD) curves for each transmission band are indicated by the solid green line in Fig. 1(b), which shows the characteristic GVD of an ARROW fiber as described in the introduction, and in more detail in Ref [8]. The confinement losses are high, ~27 dB/cm at 1600 nm, which is due to the template design not being optimal for this extreme refractive index contrast. Work is ongoing to design and fabricate a template that permits low confinement loss transmission bands for such high index contrast fibers. Despite the high confinement loss, the fiber supports a single mode in the antiresonance guidance bands and the simulated intensity profile of this mode at a wavelength of 1570 nm can be seen in Fig. 1(c). The mode profile is approximately Gaussian and the mode field diameter (MFD), full-width half-maximum at the $1/e^2$ power level, was determined to be 3.1 μm.

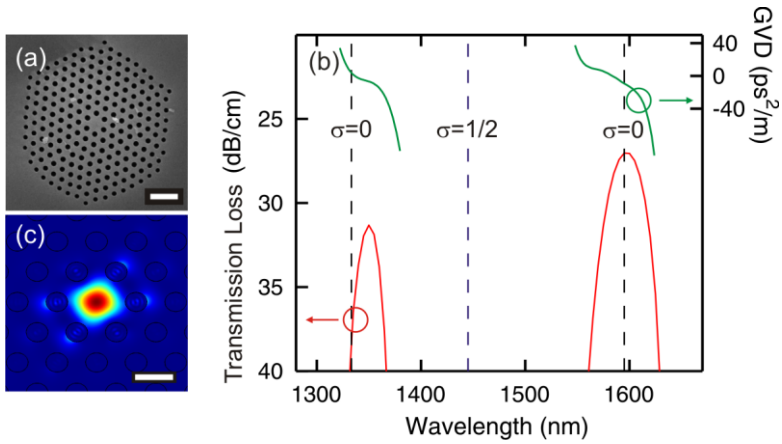

Fig. 1. (a) PCF template used for the design and fabrication of the Si-ARROW fibers, scale bar 5 μm. (b) Transmission spectrum (solid red) and GVD (solid green) of the Si-ARROW fiber, as predicted by the modal simulations, together with the resonance (dashed blue) and antiresonances (dashed black) predicted by Eq. (1). (c) The simulated intensity profile of the mode at 1570 nm, scale bar 2 μm.

The Si-ARROW fiber was fabricated by depositing a-Si:H into the capillary holes of the PCF template using the method described in Ref [13]. This deposition technique offers an additional degree of freedom for waveguide design as the semiconductor can be deposited as thin films to tune the width and position of the resonances [18], or can be doped to alter its properties for device functionality [19]. In this case we forced a silane and helium mixture to flow through the capillary holes of the silica template while it was heated in a tube furnace. The precursor decomposition could be controlled by adjusting the furnace temperature to tune the hydrogen content. The benefit of depositing the material in a-Si:H form is two-fold. Firstly, hydrogenation can saturate the dangling bonds of the amorphous material, thus reducing absorption losses. Secondly, depositing the material in an amorphous state allows the interfacial film of silicon to assume the smooth surface of the silica walls (RMS roughness of less than 0.1 nm) to reduce scattering losses incurred via reflections off the inclusions. Figure 2(a) shows a micrograph of the resulting fiber's endface after being polished using a standard technique, which confirms that all holes have been completely filled.

#144221 - $15.00 USD Received 16 Mar 2011; accepted 21 Mar 2011; published 20 May 2011
(C) 2011 OSA

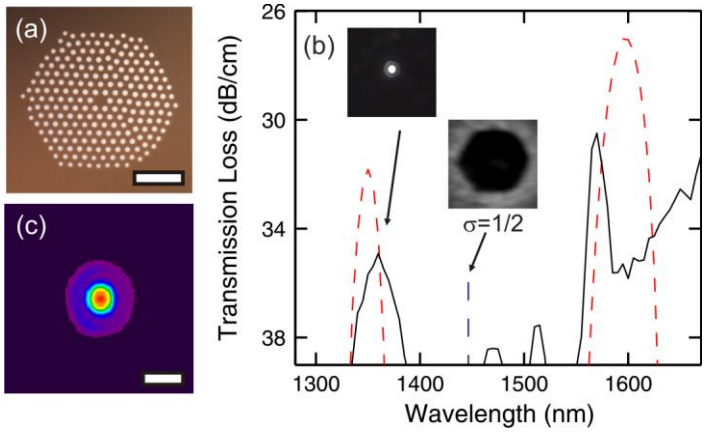

Fig. 2. (a) The polished endface of the Si-ARROW fiber, scale bar 10 µm. (b) Measured transmission spectrum (solid black) compared to the simulations (dashed red). Insets are the output images at an antiresonant condition (core guided) and at a resonant condition. (c) Measured near field intensity profile of the fundamental mode at 1570 nm, scale bar 4 µm.

In order to test the optical transmission properties of the Si-ARROW fiber, an acousto-optic tunable filter was used in conjunction with a supercontinuum source to produce an output of ~0.5 mW average power over a range of wavelengths spanning from 1300 nm to 1650 nm. The filtered light was coupled into the core of a 5 mm long fiber using a 40x microscope objective facilitated via the use of nano-positioning stages. The transmitted light was also collected using a 40x objective and focused onto an Electrophysics MicronViewer

7290A infrared camera. The core guided light was filtered from the cladding light using a pin hole. The input and core guided powers were recorded for each wavelength to define the transmission spectrum, shown as the solid black curve in Fig. 2(b). This spectrum exhibits two distinct transmission bands centered at 1365 nm and 1570 nm that match well with the FEM simulations, indicated by the dashed red curve. We note that the central bands near 1500 nm did not support a core mode, in accordance with the resonance predicted by Eq. (1) at 1450 nm, and this is confirmed by the throughput images inset in Fig. 2(b). Furthermore, we attribute the transmission measured above 1600 nm to contaminations from light that is guided in the silicon rods as the wavelength dependence of this is in accordance with the transmission characteristics of an a-Si:H core in Ref [13]. This artifact is observable due to the very short fiber length (so that the light in the silicon is not entirely depleted) and also because the large numerical aperture (and hence large exit angle) of the silicon rods means that this light cannot be entirely removed via the pin hole. Compared to the simulations, there is a clear reduction in the width of the measured transmission band at 1570 nm. This is likely to be due to variations in the indices of the inclusions and, as such, is only evident in the longer wavelength band where the light penetrates further into the cladding. The ability to withstand such variations is an important consequence of the ARROW mechanism as fibers that do not have high index cladding inclusions (e.g. silica-air PBG fibers) can suffer a total loss of guidance when their periodicity is disrupted. For our fiber, the extreme refractive index contrast between a-Si:H and silica means that the inclusions are well isolated, with the result being that the widths of the transmission bands are determined by the summation of the resonances of each individual inclusion. Therefore, variations in these resonances manifest themselves as a narrowing of the transmission bands rather that a complete breakdown of the fiber's guidance mechanism [20], thus increasing the tolerance of these fibers to fabrication imperfections. The near field intensity profile of the guided mode at 1570 nm was captured using the infrared camera, in conjunction with Spiricon's LBA software, and is shown in Fig. 2(c). The profile of the mode is approximately Gaussian with a MFD of 2.8 µm, which compares well with the 3.1 µm predicted by the simulations. To determine the transmission

#144221 - $15.00 USD Received 16 Mar 2011; accepted 21 Mar 2011; published 20 May 2011
(C) 2011 OSA

losses at the maxima of the Si-ARROW fiber's transmission bands, cut-back measurements were undertaken by polishing ~1 mm off the fiber length at each measurement. The lowest losses for the 1365 nm and the 1570 nm bands were calculated to be 35 dB/cm and 31 dB/cm, respectively, which are not too dissimilar to those estimated from the simulations where the peak transmissions are ~31 dB/cm and ~27 dB/cm. A possible explanation for the discrepancies in these losses is an underestimation of material loss in the simulations.

3. Hybrid Si-ARROW fiber

Theoretical studies have shown that confinement losses can be reduced significantly by leaving some of the outer or inner cladding holes unfilled [21]. Here we chose to leave the inner holes unfilled both to reduce the losses associated with the mode interacting with the silicon, but also because the high index of our inclusions means that the core mode is well isolated from the outer rings. This fiber design, however, yields a type of hybrid TIR/ARROW structure where the mode is primarily guided by TIR, due to the inner ring of air holes, but evanescently interacts with the high index cladding so that when the wavelength is on resonance with an inclusion mode, the light will radiate out of the core. As a result, these types of fiber offer the benefit of reduced confinement losses, whilst still maintaining some of the functionality of an ARROW fiber. The simulated transmission spectrum of the proposed hybrid Si-ARROW fiber is shown by the dashed red curve in Fig. 3(a). It is clear that the fiber retains the band structure associated with its ARROW guiding characteristics and five transmission bands with negligible confinement loss at their maxima are predicted. The solid green line in Fig. 3(a) shows the fiber's GVD as a function of wavelength and it is obvious that the fiber no longer has the characteristic GVD curves associated with an ARROW fiber, as seen in Fig. 1(b), but now exhibits a dispersion associated with the TIR guiding induced by the inner ring of air holes [21]. In particular, the curve follows that of the GVD for the silica template from 800 nm to 1200 nm but then starts to decrease dramatically for the longer wavelengths when more of the light interacts with the silicon rods. Furthermore, it is also evident from the intensity profile in Fig. 3(b) that the mode's interaction with the inner holes has been reduced, resulting in a slightly smaller estimate for the MFD of 3 μm.

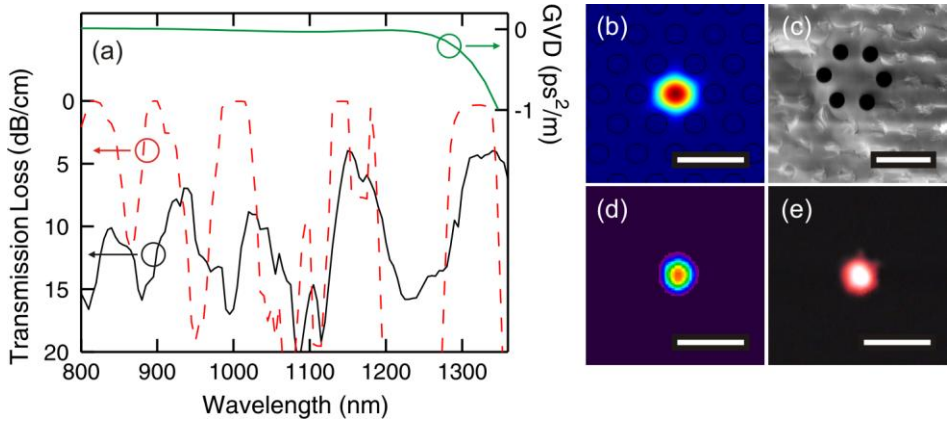

Fig. 3. (a) Measured (solid black) and simulated (dashed red) transmission spectra with the simulated GVD curve (green solid) of the hybrid Si-ARROW fiber. (b) The simulated intensity profile of the mode at 1310 nm. (c) SEM image of the fabricated fiber. (d) The measured near field intensity profile of the fundamental mode image at 1310 nm. (e) Micrograph showing a guided mode at 620 nm where the photon energy is greater than the bandgap energy of a-Si:H. All scale bars are 4 μm.

The hybrid Si-ARROW fiber was fabricated by selectively filling the PCF template with the semiconductor material. Prior to deposition, the inner holes were plugged with UV curing epoxy to prevent infiltration of the semiconductor. This was achieved by using a focused ion

#144221 - $15.00 USD Received 16 Mar 2011; accepted 21 Mar 2011; published 20 May 2011
(C) 2011 OSA

beam (FIB) to deposit a platinum mask over the holes that were to be excluded from the epoxy plugging process. The masked end of the PCF template was dipped into the epoxy and ~10 mm was drawn into the open holes via capillary action. The epoxy was then cured using an argon-ion laser and the fiber was cleaved to remove the platinum mask and expose the modified PCF template. a-Si:H was deposited into the unplugged holes using the same process as for the Si-ARROW fiber. An SEM image of the hybrid Si-ARROW fiber is presented in Fig. 3(c) which confirms both the exclusion of any material in the inner ring of holes and the complete filling of the outer holes with the semiconductor.

The hybrid Si-ARROW fiber was characterized in a similar manner to the Si-ARROW fiber, but a longer 20 mm sample was used owing to the lower predicted losses. The measured transmission spectrum of the fiber is plotted as the solid black curve in Fig. 3(a), showing good qualitative agreement with the simulations. The measured near field mode image, shown at 1310 nm in Fig. 3(d), also has a slightly reduced MFD of 2.7 μm. Cut-back measurements were used to determine the transmission losses with the lowest value being 4 dB/cm at 1310 nm, which is almost three orders of magnitude lower than that measured in the Si-ARROW fiber at 1365 nm. Here we attribute the non-negligible measured losses again to an underestimation of the material losses, and this is particularly noticeable at the shorter wavelengths which are close to the band edge. Finally, preliminary experiments have also shown that this fiber can support modes at wavelengths that have a photon energy greater than the a-Si:H valence-conduction bandgap (1.7 eV). This is illustrated in Fig. 3(e), which shows guidance at 620 nm (photon energy of 2 eV), and opens up the potential for silicon fiber devices to find use over an even broader wavelength range. Significantly, the empty pores can also be used as receptacles for the infiltration of a host of different materials which could either enhance the fiber's performance (for example, by incorporating highly non-linear organic materials) or extend their capabilities (incorporating gases or fluids for sensing).

4. Conclusion

We have designed and fabricated two silicon functionalized optical fibers which exhibit ARROW guiding characteristics by filling the holes of a TIR guiding PCF with a-Si:H. Using a selective filling technique we have shown that it is possible to modify the guidance mechanism as well as control the transmission losses. We are currently focused on optimizing the template design, semiconductor filling pattern and material properties so that future iterations will have much reduced losses. The potential to incorporate the semiconductor functionality into the fiber's cladding while maintaining guidance in the low loss silica is an important concept for the future integration of semiconductor fibers into existing fiber infrastructures. For example, we can use the electrical, thermo-optic and nonlinear properties of the semiconductor cladding inclusions to shift the bandgap for optical filtering or ultrafast modulation schemes. Furthermore, this fiber type also offers a potential solution to negate the coupling issues traditionally associated with silicon photonic devices, such as high reflection losses and nano-scale core sizes. As such, we anticipate that these fibers will become an integral part of the rapidly growing catalogue of functional semiconductor optical fibers.

Acknowledgments

The authors acknowledge EPSRC (EP/G051755/1 and EP/G028273/1), NSF (DMR-0806860) and the Penn State Materials Research Science and Engineering Center (NSF DMR-0820404) for financial support. A. C. Peacock is a holder of a Royal Academy of Engineering fellowship.

#144221 - $15.00 USD Received 16 Mar 2011; accepted 21 Mar 2011; published 20 May 2011
(C) 2011 OSA

152.78.209.172 {ts '2019-08-21 09:30:24'}